

Sample erosion studies and modeling in a glow discharge ionization cell

MARK VAN STRAATEN,* AKOS VERTES and RENAAT GIJBELS

University of Antwerp, Dept. of Chemistry, Universiteitsplein 1, B-2610 Wilrijk-Antwerp, Belgium

(Received 25 June 1990; accepted 25 September 1990)

Abstract—The etching rate of Mo samples in a planar glow discharge configuration using Ar as discharge gas is measured as a function of applied power density (0–10 W/cm²) and pressure inside the discharge cell (365–750 mTorr). These etching rates are compared with calculated values obtained by modeling of a one dimensional planar glow discharge. The structure of the cathode fall region is modeled in terms of a set of one-dimensional Boltzmann equations describing the three main particle types, ions, neutrals and electrons. Numerical solution of these equations provide the etching rate of the target and the energy distributions of the components. Satisfactory correlation between the measured and calculated etching rates allowed it to conclude also that other quantities for understanding plasma processes like the diffusion profiles of sputtered neutrals can reliably be predicted.

INTRODUCTION

IN THE last two decades, glow discharge devices have gained increasing interest in analytical spectrometry because of their ability to act as a source of atomization, excitation and ionization for solid samples [1, 2]. Atomic absorption, optical emission and mass spectrometers coupled with glow discharge devices (d.c.; pulsed d.c. or rf) are or will become powerful techniques in elemental analysis [3–9]. In mass spectrometry in particular, the recent development of double focusing and quadrupole instruments, both by commercial companies and in research laboratories, provides an alternative to more established mass spectrometric techniques. Especially the commercially available double focusing instrument (VG 9000) is expected to be the successor of spark source mass spectrometers because of its better reproducibility and comparable or even higher sensitivity [10–12].

The use of a glow discharge for the mass spectrometric analysis of solids implies the understanding of three basic phenomena that determine the analytical performance of a glow discharge cell: atomization, ionization of sample material, and ion extraction from the cell. In this paper we focus upon the atomization step; ionization and ion extraction will be the subjects of later studies. Atomization in a glow discharge (GD) is the result of cathodic sputtering and depends on three experimental parameters, current, voltage and pressure. The setting of these parameters has a pronounced effect on the sputter rate of the sample, so that careful adjustment of discharge conditions is needed for different analytical applications such as bulk analysis or depth profiling. The sputter process in a glow discharge is essentially different from sputtering in a high vacuum environment such as in, e.g. a SIMS instrument. The noble gas sputter environment in a glow discharge accounts for two major features not occurring in sputtering caused by ion bombardment. First, the mean free path of the sputtered species is small (≈ 0.1 mm, for $p=760$ mTorr), indicating that collisions between sputtered and gas species are numerous and can lead to redeposition of sputtered particles on the target. Second, owing to mainly charge exchange processes in the cathode dark space, high-energy neutral gas atoms are formed with a velocity component directed towards the sample surface. As a result, sputtering by fast atom bombardment can account for a major part of the total sputter yield, especially at high pressures.

Our aim is to arrive at a better understanding of the plasma structure and plasma processes. It is assumed that this goal is achieved if, e.g. calculated and measured

* Author to whom correspondence should be addressed.

etching rates agree. Modeling of plasma processes in atomization and ionization sources has always attracted a lot of interest (ICP, GD, spark source, laser [13]; spark source [14]). Although almost never covering completely all underlying aspects, it still yields a better knowledge of the phenomena involved. For the spectroscopist, who uses the plasma source for analytical purposes, a good basis can be built to explain his results obtained by detection of the different plasma species. In our case, this can then lead to a better control of the plasma defining parameters, resulting in more precise and accurate analytical applications of the glow discharge for mass spectrometry.

In this work we have measured the etching rate of molybdenum samples in a planar glow discharge configuration at different operating conditions. The results of these experiments were then compared with theoretical predictions of etching rates, obtained by computer modeling of a one-dimensional planar glow discharge [15]. The satisfactory correlation between calculated and experimental results justified the use of experimentally more difficult accessible quantities predicted by the theoretical calculations for understanding plasma processes and for optimization of analytical applications.

EXPERIMENTAL

Glow discharge source

The etching rate experiments were performed using the glow discharge source of the double focusing mass spectrometer VG 9000, operating in the so-called abnormal mode [16]. In this context abnormal mode is meant if an increase in current is accompanied with a sharp raise in voltage. The glow discharge cell (Fig. 1), which confines the discharge to a small volume and is mounted in the source housing, is comparable with the cell normally used for analyzing flat samples. The cell was equipped with a thermocouple gauge for measuring the pressure inside the cell. This gauge was calibrated against an absolute pressure gauge (Leybold, Membranovac 200), showing good response and sensitivity in the operating pressure range (0.35–1 Torr). A Viton O-ring between the sample and the mask of the sample holder provided extra sealing so that no gas leaking could occur through the sample holder. The sample is held against the mask by a small spring.

Argon was used as working gas, having a total impurity level $3 \times 10^{-4}\%$. The gas is introduced into the cell through a needle valve and a capillary glass tube; a gas flow rate of 0.1–0.5 ml/min

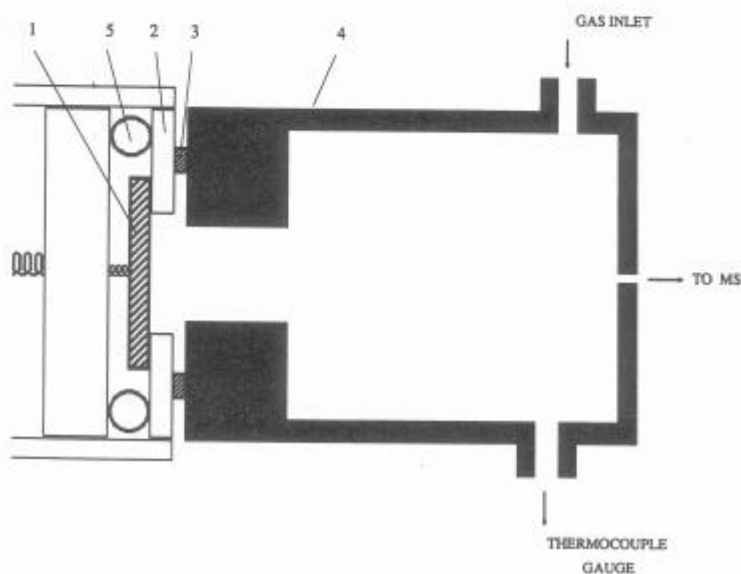


Fig. 1. Sketch of the glow discharge cell. 1 Sample (cathode); 2 Ta mask; 3 boron nitride insulator; 4 cell body (anode); 5 Viton O-ring.

yields pressures inside the GD cell between 0.1 and 1 Torr. The power supply was operated in the constant current mode at voltages up to 1300 V. During the experiments the voltage was monitored using a high voltage probe and a normal voltmeter.

The molybdenum samples (99.9% pure) were plates of approximately 17 mm by 17 mm and 1 mm thick. Before they were exposed to the plasma, they were rinsed in deionized water and dehydrated ethanol, and dried in an oven at 110°C for 1 hr. Using a test sample the pressure inside the cell was monitored without applying power to the system (heating of the cell by the plasma can cause false pressure readings since the pressure gauge is temperature dependent) and this showed that the pressure was constant within 5% during 1 hr. Each sample was sputtered for 1 hr at different operating conditions. The discharge voltage revealed no variation above 5% during the 1 hr sputter process.

Profilometer

The etching rate was not measured by weight loss but by examination of the obtained craters in the Mo samples with a stylus-type profilometer (Dektak 3030). This method, although possibly not as accurate as the weight loss method, gives extra information about the sputter process which can be deduced from the crater form.

MODELING OF A PLANAR GLOW DISCHARGE

A glow discharge is built up of a number of regions from which the cathode dark space has high significance regarding cathodic sputtering. Because sputtering and glow discharge are stationary, but strongly non-equilibrium processes, the spatial and energy distributions of the species involved have to be described by a set of transport equations. A steady state form of the one-dimensional Boltzmann equation [17] is used to describe the flux energy distributions of ions, $f_i(x, E)$, neutrals, $f_n(x, E)$ and electrons, $f_e(x, E)$:

$$\frac{\partial f_i(x, E)}{\partial x} = -e \frac{d\phi(x)}{dx} \frac{\partial f_i(x, E)}{\partial E} - \frac{f_i(x, E)}{\lambda_{ch}(E)} + \delta(E) \left[\int \frac{f_i(x, E')}{\lambda_{ch}(E')} dE' + \int \frac{f_c(x, E')}{\lambda_i(E')} dE' \right] \quad (1)$$

$$- \frac{\partial f_e(x, E)}{\partial x} = e \frac{d\phi(x)}{dx} \frac{\partial f_e(x, E)}{\partial E} - \frac{f_e(x, E)}{\lambda_i(E)} + \frac{f_e(x, E + E_i)}{\lambda_i(E + E_i)} + \delta(E) \int \frac{f_c(x, E')}{\lambda_i(E')} dE' \quad (2)$$

$$\frac{\partial f_n(x, E)}{\partial x} = \frac{f_i(x, E)}{\lambda_{ch}(E)} \quad (3)$$

where $f_j(x, E)dE$ is the number of particles j crossing an imaginary plane at x per unit area and unit time, with energies ranging from E to $E + dE$; $\lambda_{ch}(E)$ and $\lambda_i(E)$ correspond to the energy dependent mean free paths of charge exchange and ionization processes, respectively; E and E_i are the kinetic energy and the ionization energy; e is the electron charge and $\delta(E)$ denotes Dirac's delta, depending on energy. The potential distribution, $\phi(x)$, in the cathode dark space is determined by the Poisson equation:

$$\frac{\partial^2 \phi}{\partial x^2} = \frac{e}{\epsilon_0} \int \left(\frac{f_i(x, E)}{(2E/m)^{1/2}} - \frac{f_e(x, E)}{(2E/m_e)^{1/2}} \right) dE. \quad (4)$$

The extent of the dark space varies with the external conditions: discharge gas pressure, current density at the cathode and voltage across the dark space. Equations (1–4), supplemented with boundary conditions prescribing the particle fluxes and potentials at the cathode and at the dark space/negative glow interface, form the complete mathematical model. Secondary electron emission from the cathode material due to ion and neutral bombardment, and charge exchange processes for the discharge gas are also included.

Solutions of Eqns (1–4) are sought by an iterative scheme. The self-consistency of the iteration is checked by the calculation of the integral of the electric field strength over the cathode dark space, which should be equal to the applied voltage across the discharge. A detailed description of the computer code can be found in Ref. [15]. The output of the iteration includes the extent of the cathode fall region and the flux energy distributions, $f_j(x, E)$, of the components.

The total sputter yield is calculated utilizing the ion and neutral flux energy distributions at the cathode surface, the ion current density at the dark space/negative glow interface and an empirical formula for the sputtering yield [18].

To obtain the net erosion rate of the cathode, redeposition of neutrals through diffusion has to be accounted for. Indeed, a fraction of the sputtered particles after thermalization returns to

the cathode surface via a diffusion process. This can be described by the one-dimensional stationary diffusion equation [19]:

$$D \frac{\partial^2 n(x)}{\partial x^2} = -J_0 F_T(x). \quad (5)$$

The number density distribution of sputtered particles, $n(x)$, is determined by the emitted flux, J_0 , by their thermalization profile, $F_T(x)$ and by the diffusion coefficient, D . Thermalization profiles are determined for a given interaction potential and the subsequent analytical solution of Eqn (5) is used to calculate the diffusion current to the cathode. In this way one finally obtains the particle distribution in the discharge cell and the net etching rate.

RESULTS AND DISCUSSION

The operation of a glow discharge in the abnormal mode is defined by three parameters, pressure, current and voltage, of which only two can be changed independently. This means that for a given pressure a choice of current or voltage automatically fixes the other. If one makes the correlation with high vacuum sputtering, the sputter rate of a cathode sample in a GD should be dependent on the energy of the noble gas ions (and atoms) striking the cathode surface. This ion energy is determined by the operating voltage of the discharge and owing to the multiple collisions in the gas phase, the operating voltage then gives the maximum energy of an ion hitting the sample. The mean energy of the ions is much lower; for a given set of voltage and current, the pressure defines the mean free path and thus the number of collisions an ion undergoes while it is accelerated in the cathode dark space. If the voltage determines the mean energy of the bombarding ions (and atoms) for a given pressure, the effect of the current manifests itself in the number of ions hitting the surface. Both account for the sputter rate of a sample in a glow discharge.

Experimental etching rate

For three pressures the etching rate of Mo samples is measured at three currents by profilometric examination of the sample surface after one hour sputtering. Figure 2 shows an example of a crater profile obtained by GD sputtering. The steep walls and flat crater bottom indicate that sputtering at these conditions (750 mTorr, $I=4.5$ mA, $V=1205$ V) is laterally homogeneous over a large distance (≈ 9 mm). This confirms again the depth profiling abilities of a GD in both optical emission and mass spectrometry [20, 21]. Since both current and voltage determine the etching rate, the latter was measured as a function of the applied power. By measuring also the cathode area which was under the influence of the sputtering plasma (crater diameter), the power density could be calculated, i.e. the total rate of energy input per unit area of the sample surface. Figure 3 illustrates the dependency of the etching rate on the

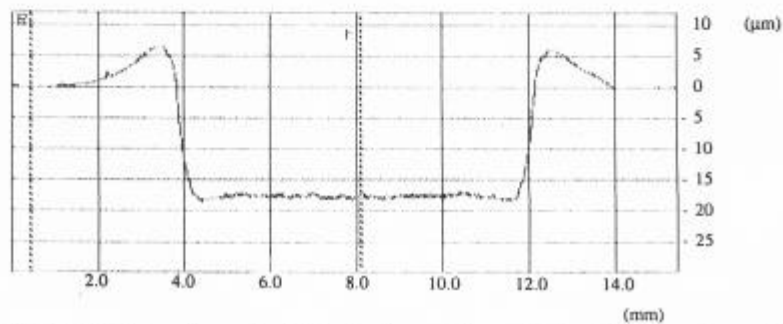


Fig. 2. Example of a crater profile obtained after one hour sputtering (Mo/Ar system, $p=750$ mTorr, $I=4.5$ mA, $V=1205$ V).

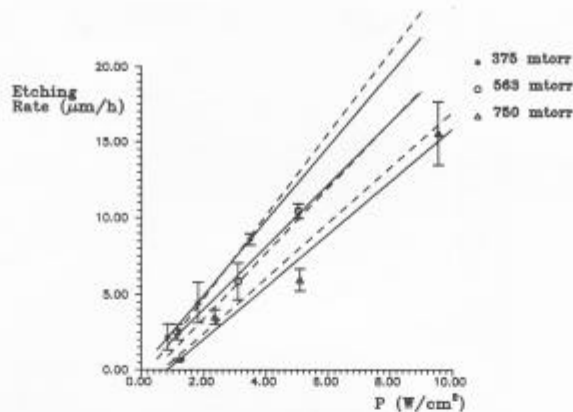


Fig. 3. Measured (—) and calculated (---) etching rates for the Mo/Ar system in a planar glow discharge as a function of applied power density for three different pressures.

applied power density, showing also the good linearity of the best fit (solid lines) for the three pressures investigated. From this figure it is obvious that higher pressures give lower etching rates at constant power density, an effect which is clearly due to the increased probability of redeposition of sputtered material onto the sample surface at higher pressures. FANG *et al.* [22] have also demonstrated this linear relationship, although they found a constant slope for the best fits over a large pressure range (between 1.5 and 8 Torr). We see here a slowly decreasing slope of the best fitted lines towards higher pressures.

Calculated etching rates

The measured etching rates at different operating conditions could be reproduced by the model calculations by introducing one fitting parameter, as is indicated in Fig. 3 by the dashed lines which correspond to the calculated values. Because of the complicated shape of the glow discharge cell and because of the presence of radial diffusion processes, we have introduced an effective sink distance in the one-dimensional model. The definition of this quantity is the distance of a perfect sink from the cathode on the cell axis, which removes just as much sputtered material from the system, as the combined effect of all the cell walls. This distance was used as the single fitting parameter to reach agreement with the experimental results. The introduction of this parameter is the consequence of the one-dimensional description and as a result the radial diffusion processes are accounted for by this effective sink.

That this sink position has a pronounced effect on the etching rate is obvious: it determines the particle diffusion current density away from and towards the sample surface. As calculated for 565 mTorr by the model, these fluxes are 24 and 72%, respectively; a finite amount of 4% of the particle flux reaches the sink position without being thermalized completely [19]. Changing the sink position changes the fractional particle diffusion towards and away from the source and thus the amount of redeposited material, resulting in a different etching rate at constant operating conditions.

Diffusion profiles of sputtered neutrals

Since the model can yield acceptable values for the etching rate, we assume that also other quantities can now reliably be predicted; this will lead to a better understanding of the plasma structure regarding the potential distribution in the cathode fall region, the atomization of sample material and the diffusion processes. Although the etching rate is the only experimental verification, it gives a good indication of the validity of the model since it is the result of the final stage of the model calculations.

One of the predicted quantities closely related to the etching rate is the diffusion profile of sputtered neutrals. Figure 4 shows the diffusion profiles of sputtered neutrals

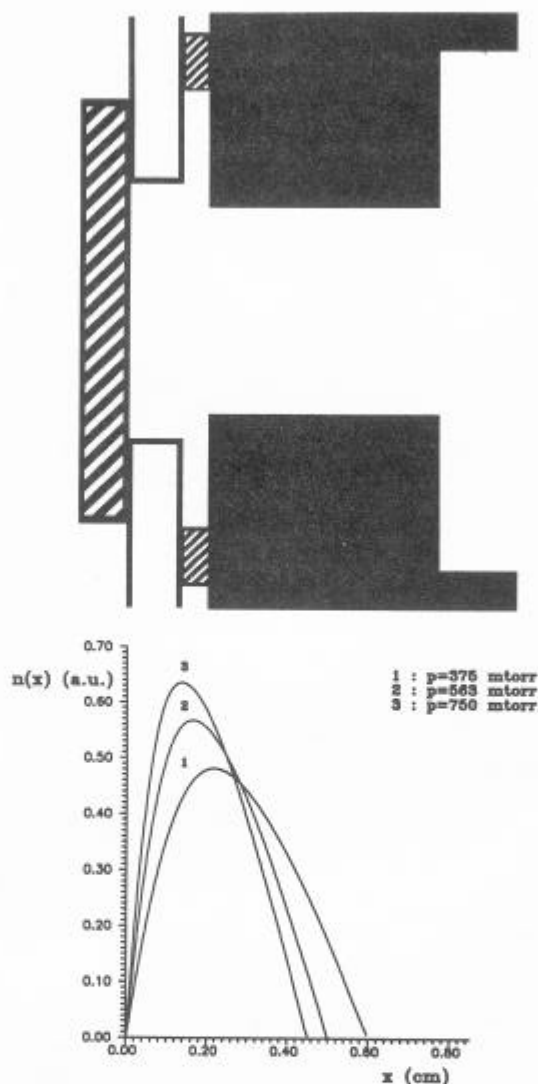


Fig. 4. Calculated diffusion profiles of sputtered neutrals in a planar glow discharge cell for three different pressures.

(after thermalization) as calculated with an effective sink distance of 6, 5 and 4.5 mm, for 375, 565 and 750 mTorr respectively, together with a part of the cell configuration drawn on the same scale. This sink distance corresponds to the fitting parameter in Fig. 3. For the pressures investigated (the applied power density has no influence on the diffusion profiles since it concerns sputtered neutral species) the diffusion profiles show a maximum just in front of the cathode sample, explained by the fact that the sample surface also acts as a sink after the sputtered neutrals are thermalized. In our experimental geometry this means heavy redeposition on the sample and inside the neck of the cell, also confirmed in reality.

The maximum of the profiles shifts slightly towards the sample surface at higher pressures. The reason for this can mainly be found in the decreasing range of thermalized particles towards higher pressures as a result of a more effective energy dissipation in the surrounding gas environment due to the increased number of collisions per atom (smaller mean free path). Since the thermalization profile is used as a source

term in the diffusion equation, also the maximum of the diffusion profile will be affected and shifted towards the sample surface.

LOVING *et al.* [23] found continuously decreasing atom number densities away from the sample surface at higher pressures, measured by atomic absorption spectrometry (AAS). The absence of a pronounced maximum in their experiments does not in the first instance contradict the calculated values here. The spatial resolution of the AAS measurement is low (≈ 1 mm) and combined with a shift of the maximum of the diffusion profile towards the sample surface at higher pressures, it is possible that only the descending part of the calculated profile has been measured accurately.

The study of the distribution of sputtered atoms in a Grimm-type glow discharge configuration by FERREIRA *et al.* [24] also showed distribution profiles with a maximum close to the cathode surface. The diffusion model used by these authors could not explain this phenomenon and they attributed the maximum to the sputtering of clusters from the sample surface (see also Ref. [25]). These clusters are not detectable by atomic absorption measurements until they are dissociated in the plasma by one of the numerous possible collision processes. The diffusion model used here differs however substantially from the one elaborated by FERREIRA *et al.* They identified the flux of sputtered sample atoms moving away from the sample surface with the sputter rate of the sample, and assumed that the sputtered particles have thermal energies when they are introduced into the plasma at the cathode surface. In this way, redeposition on the cathode is neglected and the cathode cannot act as a sink in the diffusion model. This condition largely contradicts our estimates of the back-diffusion current.

Other authors reported a peaked spatial distribution of sputtered atoms, but found an explanation in the increased degree of ionization in the cathode dark space by high energy electron impact [26]. CHAPMAN [16], on the other hand, stated that ionization in the sheath is minor compared to ionization in the negative glow region.

CONCLUSION

The etching rate of Mo samples in a planar glow discharge configuration shows a linear dependency on the applied power density. The one-dimensional model used to describe the planar glow discharge is in accordance with the etching rate experiments: one fitting parameter allows us to reproduce the measured etching rates by the model calculations. Valuable information regarding the plasma structure and fundamental processes occurring in the discharge can be drawn from the model, although several calculated quantities should be checked further by experiment.

Calculated diffusion profiles of sputtered neutrals illustrate that the abundance of neutral atoms is the highest just in front of the sample. As a consequence of diffusion towards and away from the sample surface (after thermalization), the profiles are peaked; the profile maximum shifts towards the sample at higher pressures.

Although in this stage the work is still tentative, better cell design can be aimed at by better understanding of sputtering and diffusion processes in a glow discharge.

Acknowledgements—The authors wish to thank I. ABRIL for her advice and help in implementing the computer code. M. VAN STRAATEN is indebted to the Instituut tot Aanmoediging van Wetenschappelijk Onderzoek in de Nijverheid en Landbouw (IWONL) for financial support. This publication forms part of research results in a project initiated by the Belgian State-Prime Minister's Office-Science Policy Programming.

REFERENCES

- [1] W. W. Harrison, *J. Anal. At. Spectrosc.* **3**, 867 (1988).
- [2] F. Adams, R. Gijbels and R. Van Grieken, Eds, *Inorganic Mass Spectrometry*. Wiley, New York (1988).
- [3] M. R. Winchester and R. K. Marcus, *Appl. Spectrosc.* **42**, 941 (1988).
- [4] C. G. Bruhn and W. W. Harrison, *Anal. Chem.* **50**, 16 (1978).
- [5] J. A. C. Broekaert, *J. Anal. At. Spectrosc.* **2**, 537 (1987).

- [6] W. W. Harrison, K. R. Hess, R. K. Marcus and F. L. King, *Anal. Chem.* **58**, 341 (1986).
- [7] N. Jakubowski, D. Stuewer and W. Vieth, *Anal. Chem.* **59**, 1825 (1987).
- [8] J. A. Klinger, P. J. Savickas and W. W. Harrison, *J. Am. Soc. Mass Spectrom.* **1**, 138 (1990).
- [9] D. C. Duckworth and R. K. Marcus, *Anal. Chem.* **61**, 1879 (1989).
- [10] L. F. Vassamillet, *J. Anal. At. Spectrom.* **4**, 451 (1989).
- [11] R. Gijbels, *Talanta* **37**, 363 (1990).
- [12] F. Adams and A. Vertes, *Fresenius' J. Anal. Chem.* **337**, 638 (1990).
- [13] A. Vertes, R. Gijbels and F. Adams, *Mass Spectrom. Rev.* **9**, 71 (1990).
- [14] M. van Straaten, A. Vertes and R. Gijbels, *Anal. Chem.* **62**, 1825 (1990).
- [15] I. Abril, *Comp. Phys. Comm.* **51**, 413 (1988).
- [16] B. Chapman, *Glow Discharge Processes*. Wiley, New York (1980).
- [17] N. W. Ashcroft and N. D. Mermin, *Solid State Physics*, pp. 319–320. Holt, Reinhart and Winston, New York (1976).
- [18] Y. Yamamura, N. Matsunami and N. Itoh, *Radiat. Eff.* **71**, 65 (1983).
- [19] J. A. Valles-Abarca and A. Gras-Marti, *J. Appl. Phys.* **55**, 1370 (1984).
- [20] J. Pons-Corbeau, J. P. Cazet, J. P. Moreau, R. Berneron and J. C. Charbonnier, *Surf. Interf. Anal.* **9**, 21 (1986).
- [21] M. Hecq, A. Hecq and M. Foutignies, *Anal. Chim. Acta* **155**, 191 (1983).
- [22] D. Fang and R. K. Marcus, *Spectrochim. Acta* **43B**, 1451 (1988).
- [23] T. J. Loving and W. W. Harrison, *Anal. Chem.* **55**, 1523 (1983).
- [24] N. P. Ferreira and H. G. C. Human, *Spectrochim. Acta* **36B**, 215 (1981).
- [25] A. J. Stirling and W. D. Westwood, *J. Phys. D* **4**, 246 (1971).
- [26] C. Van Dijk, B. W. Smith and J. D. Winefordner, *Spectrochim. Acta* **37B**, 759 (1982).